Dependence of the properties of titanium-pillared clays on the host matrix: a comparison of montmorillonite, saponite and rectorite pillared materials

Fathi Kooli, Janet Bovey and William Jones*

Department of Chemistry, Cambridge University, Lensfield Road, Cambridge, UK CB2 1EW

Titanium pillared clays using montmorillonite, saponite and rectorite hosts have been prepared from $TiCl_4$–ethanol solutions. The products have been characterised structurally by PXRD and IR studies and for acidity by cyclohexylamine and pyridine adsorption–desorption studies. Catalytic activity data for pentanol dehydration and cumene cracking are also presented. The amount of Ti incorporated is related to the cation-exchange capacity of the host. The thermal stability of the pillared material decreases from rectorite through montmorillonite to saponite. Cyclohexylamine desorption suggests that the saponite sample has the highest acidity, and this is reflected in the highest conversion for cumene cracking. In the case of pentanol dehydration, however, the highest activity is seen for the rectorite sample, despite its apparent lower acidity. Similar effects have been reported previously for this reaction with alumina pillared clays.

A variety of metal oxides may be incorporated into the interlayer space of clays to generate expanded high surface area porous solids.[1–8] The thermal stability, adsorption properties and catalytic activities of these so-called pillared clays have been studied extensively,[9–11] particularly those in which the host matrix is a montmorillonite clay and the pillaring agent is a polymeric hydroxyaluminium cation.[12]

The microstructure of the resulting pillared materials obtained after calcination of the exchanged clay is dependent on, amongst other factors, the nature of the host lattice,[12,13] the nature of the pillar[14–17] and the preparation conditions.[18,19] Alumina-pillared clays have been shown to be predominantly microporous,[18,20] while titania-[21] and gallium-pillared clays[22] exhibit significant amounts of mesoporosity.

Titanium oxides have several significant properties as catalyst supports.[23] Yoneyama *et al.*[24] have investigated the photocatalytic properties of TiO_2 when incorporated as pillars in montmorillonite and found the activities to be greater for the pillared clay than for TiO_2 powder particles in the decomposition of propan-2-ol and a number of carboxylic acids. Despite these promising properties, however, titania-pillared materials are frequently poorly ordered compared to their alumina counterparts, thus making the establishment of sample reproducibility difficult.[25,26]

This paper investigates the properties of montmorillonite, saponite and rectorite clays pillared with TiO_2, and presents acidity and catalytic activity data for these materials. Montmorillonite is a dioctahedral smectite which possesses a negative layer charge arising primarily from the substitution of magnesium and/or iron for aluminium in the octahedral manifold. Saponite differs from montmorillonites in that it has a negatively charged tetrahedral manifold (resulting from the replacement of silicon by aluminium) similar to that in beidellite. Rectorite is a mixed-layer clay composed of regularly 1 : 1 interstratified low charge montmorillonite-like layers and high charge density (non-expandable) mica-like dioctahedral layers.[27]

The pillared materials described here were prepared using the procedure described by Lin *et al.* which utilises a $TiCl_4$–ethanol solution mixed with glycerol and water.[26] This method has been used to prepare a variety of Ti-pillared materials, including acid-activated clays.[25,28]

Experimental

Starting materials

The raw clays were used as received. A Peruvian montmorillonite was supplied by Laporte Industries Ltd. (Widnes, UK). The clay had a cation-exchange capacity (CEC) of 91 mequiv $(100\ g\ clay)^{-1}$ and the following structural formula $Ca_{0.24}[Si]_4[Al_{1.40}Fe_{0.1}Mg_{0.39}]O_{10}(OH)_2$.[29] A saponite clay was obtained from the Source Clay Repository, Columbia, USA. The composition is given as: $(Na_{0.27}Ca_{0.05})(Mg_{2.87}Fe_{0.09})(Si_{3.63}Al_{0.37}O_{10})(OH)_2$. The corresponding CEC is 79 mequiv $(100\ g\ clay)^{-1}$.[30] A natural rectorite was obtained from W. R. Grace & Co, Columbia. It had a CEC of 50 mequiv $(100\ g\ clay)^{-1}$ and the unit cell composition was $[K_{0.23}Na_{0.33}Ca_{0.39}](e)[Ca_{0.19}Mg_{0.01}](ne)[Al_{3.91}Mg_{0.09}O_6](oh)[Si_{6.03}Al_{1.68}Ti_{0.29}O_{16}](td)$ classified into exchangeable ions (e), non-exchangeable ions (ne), octahedral sheet (oh) and tetrahedral sheet (td).[31]

Pillaring procedure

The pillaring agent was prepared using the method described by Lin *et al.*[26] $TiCl_4$ (Aldrich) was mixed with twice the volume of ethanol and stirred until a homogeneous, yellow solution was obtained. Five millilitres of this solution was added to a mixture of 25 ml of deionized water and 25 ml of glycerol. The resulting clear mixture was then stirred for 3 h, and subsequently added dropwise to a rapidly stirred suspension of 2.5 g of clay in 250 ml of deionized water [*i.e.* 6 mmol Ti (g of clay)$^{-1}$]. After further stirring for 4 h, the precursor-pillared clay was separated by filtration and washed with deionized water until chloride free and dried at room temperature. The precursor-pillared materials were calcined at 500 °C for 4 h in air to give the Ti-pillared products.

Characterisation of the materials

Elemental analyses were performed on a Philips PW 1400 X-ray fluorescence spectrometer fitted with a rhodium target. Powder X-ray diffraction (PXRD) patterns were recorded using a Philips APD 1700 instrument, with Ni-filtered Cu-Kα radiation and a step of 0.02°. Surface areas, pore volumes and pore size distributions were obtained using a Micromeritics ASAP 2000 porosimeter. The samples were degassed under vacuum for 3 h at 200 °C prior to analysis.

Brønsted acidity (proton concentration) was determined using thermogravimetry (TG) of the clays following cyclohexylamine desorption.[32] The mass loss between 290 and 420 °C was used to compute the acidity in terms of mmol of cyclohexylamine desorbed.

The Fourier-transform IR (FTIR) spectra of chemisorbed pyridine were measured using a Nicolet 205 FTIR spectrometer. The material (40–50 g), previously calcined in air for

4 h at 500 °C, was pressed (for 2 min at 10 ton cm^{-2} pressure under vacuum) into a self-supporting wafer 13 mm in diameter. The wafer was further calcined under vacuum (10^{-3} Torr) at 500 °C for 2 h and then exposed to pyridine vapour at ambient temperature before being heated at 100 °C for 1 h (while still in the pyridine atmosphere) to allow the pyridine to permeate the sample. The wafer was cooled to ambient temperature and evacuated for 1 h. The wafer was then heated for 1 h at temperatures between 100 and 500 °C, with further spectra being recorded at ambient temperature.

The catalytic activity of the pillared clays was investigated using as test reactions the dehydration of pentan-1-ol and cumene cracking/dehydrogenation. For dehydration of pentan-1-ol, similar reaction conditions to those reported previously were chosen.[33] The pillared clay (0.3 g) and 3 ml of pentan-1-ol were mixed in stainless-steel batch reactors which were then sealed and heated (without stirring) at 200 °C for 4 h. The reaction was subsequently stopped by immersion of the reactors in ice. A Carlo Erba HRGC 5300 Mega series gas chromatograph was used to analyse the products.

A pulsed microreactor was used for the cumene conversion reaction. The catalyst bed (0.050 g; 30–60 mesh) was activated for 1.5 h at 500 °C under a helium flow (25 ml min^{-1}). The volume of the cumene pulse was 2 μl (14.4 μmol). Products were separated and analysed with the gas chromatograph on line with the microreactor.

Results and Discussion

Amount of titanium incorporated

Chemical analyses of the precursors prepared from the three different clays are presented in Table 1. The amount of titanium incorporated is seen to depend on the host clays, with the highest amount of Ti being incorporated by the montmorillonite. The rectorite sample incorporates the lowest amount with an intermediate value for the saponite. This trend suggests that the amount of incorporated Ti is related to the cation exchange capacity of the host clay. The order of CEC values for the three clays is montmorillonite, 91 > saponite, 79 > rectorite, 50.

PXRD and thermal stability

The PXRD patterns of the titanium exchanged clays after calcination for 4 h at different temperatures are presented in Fig. 1, 2 and 3. The PXRD patterns of the raw clays are shown for comparison.

After incorporation of titanium into the montmorillonite, the PXRD pattern indicates the formation of a new phase with the d_{001} reflection at 19.40 Å [Fig. 1(b)]. By subtracting the thickness of the basal aluminosilicate layer (*ca.* 9.6 Å), the pillar height is calculated to be *ca.* 9.8 Å. This value is close to that reported previously for the incorporation of titanium polynuclear clusters.[26, 28] 002 and 003 reflections are observed clearly. Fig. 1(c) and (d) show the PXRD patterns after calcination at 500 and 700 °C, and indicate that the pillared layered structure is stable with d_{001} reflections at 18.20 and 17.86 Å,

Table 1 Chemical analysis data (mass%) of the clays obtained after the intercalation of titanium

composition	montmorillonite	saponite	rectorite
SiO_2	63.44	54.9	46.64
Al_2O_3	14.06	4.13	34.06
MgO	3.77	22.75	0.31
Fe_2O_3	1.78	1.20	0.91
TiO_2	16.95	14.20	8.87
Na_2O	trace	trace	5.25
K_2O	trace	0.31	1.31
CaO	trace	trace	2.60

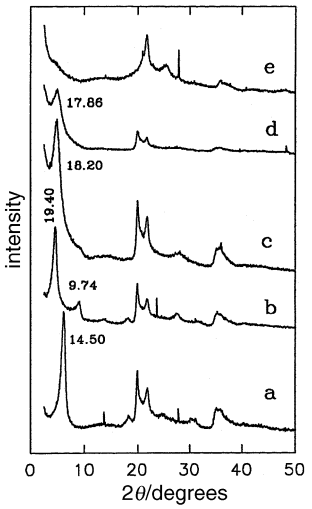

Fig. 1 PXRD patterns of (a) the raw montmorillonite and (b) after intercalation of titanium; (c), (d) and (e) correspond to sample (b) calcined at 500, 700 and 850 °C, respectively

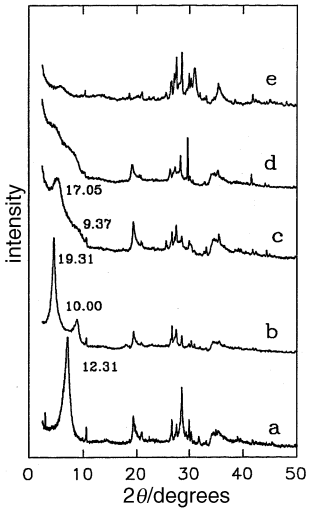

Fig. 2 PXRD patterns of (a) the raw saponite and (b) after intercalation of titanium; (c), (d) and (e) correspond to sample (b) calcined at 500, 700 and 850 °C, respectively

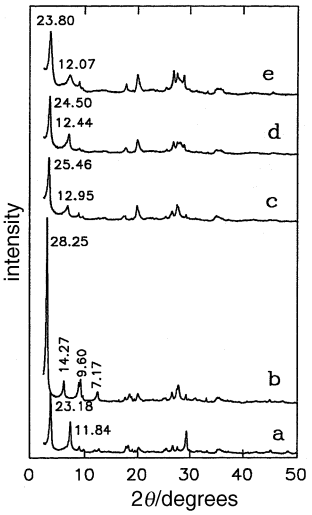

Fig. 3 PXRD patterns of (a) the raw rectorite and (b) after intercalation of titanium; (c), (d) and (e) correspond to sample (b) calcined at 500, 700 and 850 °C, respectively

respectively. We note that these values are lower than usually reported for Ti-pillared materials not using gylcerol.[34–37] After thermal treatment at 850 °C, however, no reflection is observed in the small-angle region, indicating collapse of the layered structure [Fig. 1(e)].

Fig. 2(b) indicates that for the saponite clay after titanium intercalation the 001 reflection moves from 12.31 Å to 19.31 Å, which is similar to that for the montmorillonite. After calcination at 500 °C, the PXRD pattern [Fig. 2(c)] shows that the 001 reflection is shifted to 17.05 Å, and its intensity is decreased compared to that of the precursor sample. Upon calcination at temperatures higher than 500 °C, the layer structure is destroyed progressively, and broad reflections are observed [Fig. 2(d) and (e)]. Malla and Komarneni[30] and Chevalier *et al.*[38] have reported that an alumina-pillared saponite is stable with an 001 reflection still present after calcination at 700 °C. Our observations suggest an apparent difference in thermal stability between Ti-saponites and Al-saponites.

The rectorite intercalated with the titanium complexes [Fig. 3(b)] exhibits a series of 00l reflections, *i.e.* 001, 002, 003 and 004 at 28.25, 14.27, 9.60 and 7.17 Å, respectively. Since the 'layer thickness' of the rectorite clay is *ca.* 19.2 Å, a gallery distance of *ca.* 9 Å is obtained which is similar to that obtained for montmorillonite and saponite samples. When the precursor is calcined at 500 °C, the 001 reflection shifts to 25.46 Å and its intensity decreases [Fig. 3(c)]. The PXRD patterns of the pillared rectorite treated at 700 and 850 °C show well defined 001 reflections at 24.5 and 23.8 Å [Fig. 3(d) and (e)], indicating that although contraction of the gallery height occurs the product remains well ordered. These results are to be compared with those for an Arkansas rectorite described by Bagshaw and Cooney which yielded a product giving a diffuse X-ray powder pattern.[39]

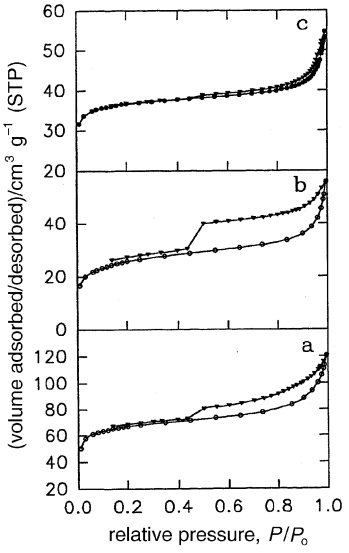

Fig. 4 Nitrogen adsorption (●)–desorption (▼) isotherms of (a) montmorillonite, (b) saponite and (c) rectorite intercalated with titanium

Surface area and porosity

Nitrogen sorption isotherms of the titanium-exchanged montmorillonite, saponite and rectorite samples are presented in Fig. 4. The shapes of the isotherms are composite type I and type IV isotherms. For the montmorillonite and saponite samples the desorption branch does not join the adsorption curve even at low relative pressures, possibly because of the irreversible adsorption of nitrogen on the aluminosilicate layers (pore walls). The hysteresis loops are of type H4 indicating the presence of narrow slit-like micropores.[40]

Table 2 shows the total BET and micropore surface areas, pore volumes and average pore diameters for the titanium-exchanged clays before and after calcination at 500 °C. In the case of montmorillonite, the total surface area (*ca.* 230 m^2 g^{-1}), the percentage of surface area arising from micropores (*ca.* 67%) and the total pore volume are similar before and after calcination. The average pore diameter is in the range typical for pillared montmorillonites.

In the case of saponite, the surface area before calcination is significantly lower (90 m^2 g^{-1}) than that of the montmorillonite. The micropore surface area is also low, at *ca.* 41%. Although an expanded material is obtained, the interlamellar space appears to be blocked, with nitrogen molecules not able to access the interlayer gallery. This is confirmed by the low total pore volume of *ca.* 0.08 cm^3 g^{-1}. After calcination at 500 °C, the surface area and the percentage of micropore volume decrease further to 54 m^2 g^{-1} and 29%, respectively.

The precursor-pillared rectorite clay exhibits a lower surface area (141 m^2 g^{-1}) compared to the equivalent montmorillonite sample. We note also that this value is lower than that reported for the same rectorite pillared with aluminium.[31] The contribution to the surface area from micropores, however, is high, at *ca.* 84%. Typically, ordered aluminium-pillared montmorillonites have surface areas in the range 300–400 m^2 g^{-1}. If only half of the silicate layers can be expanded (as in the case of interstratified rectorite), surface area values in the 150–200 m^2 g^{-1} range are to be expected for an ordered pillared rectorite.

After calcination at 500 °C, both the total surface area and the micropore surface area decrease to 98 and 76 m^2 g^{-1}, respectively, perhaps as a result of the reduced d_{001} spacing. The average pore diameter in the precursor is 19.5 Å. After calcination this value increases to 25 Å, possibly resulting from an increase in the distance between the dehydroxylated titanium polycation pillars during the thermal treatment. The partial loss of micropore volume in the calcined material may result from a distortion of the lamellar structure during the thermal treatment, such that the pores in the interior of the material become inaccessible to nitrogen.

Table 2 Total and micropore surface areas and pore volumes, and average pore diameters of the obtained samples before and after calcination at 500 °C

sample[a]	total BET surface area/m^2 g^{-1}	micropore surface area[b]/m^2 g^{-1}	total pore volume/cm^3 g^{-1}	micropore volume[b]/cm^3 g^{-1}	av. pore diameter/Å
precursor-M	229	154 (67)	0.17	0.07 (41)	22.5
pillared-M	231	153 (66)	0.18	0.07 (39)	23.6
precursor-S	90	37 (41)	0.08	0.02 (25)	25.0
pillared-S	54	16 (29)	0.05	0.01 (20)	36.0
precursor-R	141	118 (84)	0.08	0.05 (62)	19.5
pillared-R	98	76 (78)	0.06	0.03 (50)	25.5

[a]M = montmorillonite, S = saponite and R = rectorite. Precursor corresponds to Ti-exchanged sample and pillared to material obtained after calcination in air for 4 h at 500 °C. [b]Figures in parentheses are the micropore components of the surface area or the pore volume expressed as a percentage of the total surface area or pore volume.

Table 3 Acidity and catalytic activity for Ti-pillared clays using the dehydration of pentan-1-ol as a test reaction

sample	acidity[a]/ (mmol H^+) g^{-1}	pentanol converted (%)	pentene/total ethers[b]
montmorillonite	0.45 (0.37)	68	0.99
saponite	0.60 (0.28)	63	0.42
rectorite	0.46 (0.19)	83	2.2

[a]Figures in parentheses are the corresponding values for the raw clays calcined at 500 °C. [b] Pentene/ethers ratios are the molar ratios of pentene to the sum of 1,1-dipentyl ether and 1,2-dipentyl ether.

Acidity characterisation

Brønsted acidity. Table 3 presents the numbers of Brønsted acid sites obtained using cyclohexylamine as the probe molecule. The acid sites measured by this method are those accessible and strong enough to interact with the base. It is assumed that each molecule of the base interacts with one protonic (Brønsted) acid site.[32] For all samples, the number of acid sites in the Ti-pillared clay calcined at 500 °C is higher than that of the corresponding non-pillared clay also calcined at 500 °C. Ti-pillared saponite has the highest number of Brønsted sites (0.60 H^+ per g of clay at 290 °C), with montmorillonite and rectorite possessing similar, but fewer, sites. It has been reported in the case of acid-activated montmorillonite clays[41] that the surface area accessible to cyclohexylamine is a significant factor in determining the acidity of these materials. From our data, however, whilst the pillared montmorillonite exhibits a higher surface area than the pillared rectorite, the number of accessible acid sites is similar for both clays.

Brønsted and Lewis acidity. Fig. 5, 6 and 7 present the FTIR spectra following the evolution of adsorbed pyridine degassed at different temperatures under vacuum from the surface of the Ti-pillared clays.

For the montmorillonite sample at 100 °C (Fig. 5), the main vibration bands arising from the adsorbed pyridine are those bound on Lewis acid sites (L) which are observed at 1445 and 1612 cm^{-1} and those at 1545 and 1640 cm^{-1} which are assigned to pyridine on Brønsted acid sites (B). [42, 43] The strong band at 1490 cm^{-1} is attributed to pyridine associated with both Lewis and Brønsted acid sites (L + B).[42] After evacuation at 200 °C, a significant amount of pyridine remains adsorbed on both Brønsted and Lewis acid sites of the montmorillonite clay. After degassing at 300 °C, the intensities of the Brønsted bands at 1545 and 1640 cm^{-1} are reduced significantly. The intensities of the bands assigned to pyridine adsorbed on Lewis sites at 1610 and 1440 cm^{-1}, however, are still significant. Neither Brønsted nor Lewis bands are detected at 400 °C or above. New broad bands (N) at 1480 and 1430 cm^{-1} are observed which do not correspond to known vibrational bands of adsorbed pyridine. Their presence may suggest decomposition of the pyridine, similar to that observed on a Cu exchanged zeolite[44].

For the saponite sample, the spectra at 100 and 200 °C are similar to those for the montmorillonite. The spectrum after outgassing at 300 °C, however, exhibits a stronger band due to pyridine bound on Brønsted sites than the equivalent montmorillonite clay. The intensity of the Lewis band at 1445 cm^{-1} is lower than that of the L + B band at 1490 cm^{-1}, indicating that the surface of the Ti-pillared saponite exhibits both Brønsted and Lewis sites at 300 °C. The intensities of the B and L bands continue to decrease as the temperature is increased to 500 °C, although the broad bands associated with the decomposition product are still detected.

Fig. 7 corresponds to the pyridine desorbed at 200 °C on the Ti-pillared rectorite clay. It can be seen that the intensity

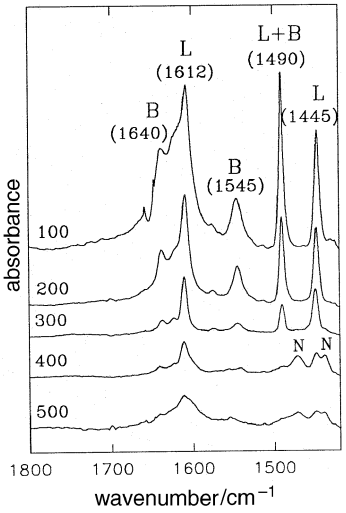

Fig. 5 FTIR spectra of pyridine adsorption on Ti-pillared montmorillonite, followed by outgassing at different temperatures (in °C). B and L correspond to pyridine bound to Brønsted and Lewis acid sites, respectively. L + B is attributed to pyridine bonded to both Brønsted and Lewis acid sites; N denotes a new band resulting from the decomposition of pyridine (see text).

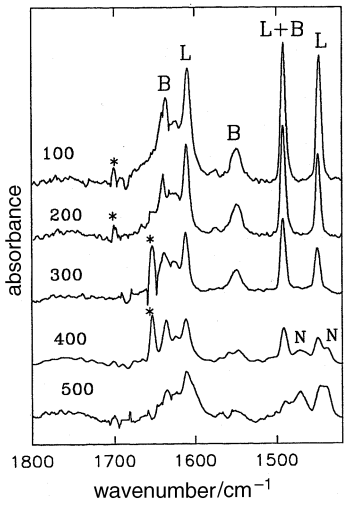

Fig. 6 FTIR spectra of pyridine adsorption on Ti-pillared saponite, followed by outgassing at different temperatures (in °C). Bands marked * are due to poor subtraction of background spectra.

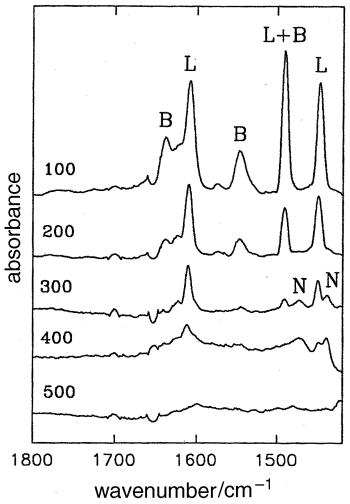

Fig. 7 FTIR spectra of pyridine adsorption on Ti-pillared rectorite, followed by outgassing at different temperatures (in °C).

of the Brønsted band (at 1548 cm^{-1}) decreases compared to 100 °C. At 300 °C all Brønsted acidity appears to be lost although a small amount of Lewis acidity remains. At 400 °C, broad bands are observed which disappear completely at 500 °C, indicating the absence of any pyridine species on the surface.

The extent to which pyridine molecules remain on acid sites at elevated temperatures reflects both the strength and the number of the surface acid sites. From our results, it appears that the Ti-pillared saponite clay has stronger Brønsted acid sites able to bind pyridine at relatively high temperature. In the case of the Ti-pillared montmorillonite and rectorite clays, the surface acidity is mainly of the Lewis acid type and few Brønsted sites are detected at temperatures higher than 200 °C.

Catalytic properties

Pentan-1-ol dehydration. The ability of the Ti-pillared clays to act as acid catalysts was investigated using the dehydration of pentanol as a test reaction. In the presence of Brønsted acid sites, pentanol is dehydrated to form a mixture of products with the major constituents being pentene, 1,1-dipentyl ether and 1,2-dipentyl ether.[45]

Table 3 shows the percentage of pentan-1-ol conversion achieved by the different Ti-pillared clays. The selectivity of the products is shown also. The highest conversion (83%) is obtained with Ti-pillared rectorite. The Ti-pillared montmorillonite and saponite clays have similar pentanol conversions (68 and 63%, respectively). These results are surprisingly different from what is expected, considering that the acidity of the Ti-pillared rectorite (as measured by the thermal desorption of cyclohexylamine) is lower than that of the Ti-pillared saponite clay. Similar behaviour is observed for this reaction over Al-pillared acid-activated clays (PAACs). The acidities of PAACs (measured by desorption of cyclohexylamine) is high, although their activity for pentanol conversion is relatively low.[29]

The product distribution indicates that the Ti-pillared saponite has a low selectivity to pentene (pentene/ether ratio = 0.42), whilst in the case of Ti-pillared rectorite, the formation of pentene is favoured (ratio = 2.2). The Ti-pillared montmorillonite exhibits an intermediate selectivity for pentene formation. The dehydration of pentanol to ethers has been reported to be related to the strength of the Brønsted acid sites on the surface of the catalyst.[45] The selectivity data in Table 3 could indicate that the Ti-pillared saponite has high Brønsted acidity with low selectivity to pentene formation. On the other hand, for Ti-pillared rectorite, the formation of pentene is favoured, with only minor transformation of pentene to ethers, thus indicating the weakness of the Brønsted acid sites on this catalyst. Ti-pillared montmorillonite exhibits intermediate behaviour with acid sites which are stronger than those of the Ti-pillared rectorite, but weaker than those of the Ti-pillared saponite. The general trend, therefore, for the alkene/ethers ratio is in agreement with the Brønsted acidity data as determined by pyridine adsorption. Delcastillo and Grange[36] have reported on the dehydration of butan-1-ol on Ti-pillared montmorillonites. High activity was obtained although, as in our case, the origin of the acid sites could not be identified unambiguously. Protons from hydroxy species associated with the titania pillar may be involved as well as some synergistic effect between titanium oxide and silicon from the sheets.

Cumene cracking and dehydrogenation. The conversion of cumene is a model reaction for identifying the Lewis/Brønsted acid site ratio of a catalyst; cumene is cracked to benzene and propene over Brønsted acid sites, whereas dehydrogenation to α-methylstyrene occurs over Lewis acid sites. The relative amounts of benzene and α-methylstyrene in the product mixture can therefore be a good indication of the types of acidities possessed by the catalyst.[46]

Table 4 Cumene hydrocracking results over various Ti-pillared clays at different temperatures

	conversion[a] (%)		
sample	300 °C	400 °C	500 °C
montmorillonite	—	2.60 (4.9)	14.00 (8.6)
saponite	8.00 (15.3)	23.50 (14.0)	62.00 (16.5)
rectorite	0.40 (1.0)	1.70 (1.6)	17.40 (3.5)

[a]Figures in parentheses are the ratio of benzene yield to α-methylstyrene yield.

The results for the Ti-containing materials are summarized in Table 4. The values shown were determined after several pulses during which the conversion stabilized. The Ti-pillared saponite has a significantly higher conversion than the montmorillonite and rectorite samples, in agreement with the acidity values measured by desorption of cyclohexylamine. In particular, the ratio of benzene to methylstyrene also appears to follow the trends seen in the pyridine desorption measurements as well as for Ti-pillared montmorillonite and beidellite. [37] For the saponite sample, for example, at 500 °C the high conversion and significant cracking activity reflect the higher Brønsted acidity seen for these materials.

Conclusions

We have reported that the preparation of three Ti-pillared clays has been achieved successfully, and that the amount of titanium intercalated between the layers is related to the cation exchange capacity of the parent clay. The thermal stability of these pillared materials depends strongly on the nature of the host clays, with the Ti-pillared rectorite being stable to 850 °C. The Ti-pillared saponite host collapses at 500 °C, and the Ti-pillared montmorillonite is stable to 700 °C. The Ti-pillared saponite has the highest acidity (as measured by cyclohexylamine desorption) and a high conversion of cumene to benzene is obtained. The dehydration of pentanol, however, is favoured more over the Ti-pillared rectorite. The Ti-pillared montmorillonite shows intermediate behaviour for these test reactions. It is likely, therefore, that the use of titanium as a pillaring species may be optimised by the appropriate choice of the starting clay matrix.

We are grateful to the EPSRC and Laporte Industries Ltd. for support of this work. The determination of surface area and porosity data by Laporte is also appreciated. Useful discussions with Dr. R. Mokaya are gratefully acknowledged. Funding by the EC through the Concerted European Action on Pillared Layered Solids (CEA-PLS) is also appreciated. We are grateful to Dr. J. Wu (W. R. Grace), for supplying a sample of rectorite clay.

References

1 G. W. Brindley and R. E. Sempels, *Clay Miner*., 1977, **12**, 229.
2 M. L. Occelli and R. M. Tindwa, *Clays Clay Miner*., 1983, **31**, 22.
3 R. Burch and C. I. Warburton, *J. Catal*., 1986, **97**, 503.
4 S. Yamanaka and G. W. Brindley, *Clays Clay Miner*., 1979, **27**, 119.
5 G. W. Brindley and S. Yamanaka, *Am. Mineral*., 1979, **64**, 830.
6 M. S. Tzou and T. J. Pinnavaia, *Catal. Today*, 1988, **2**, 243.
7 S. Yamanaka, T. Doi, S. Sako and M. Hattori, *Mater. Res. Bull*., 1984, **19**, 161.
8 J. M. Oades, *Clays Clay Miner*., 1984, **32**, 49.
9 D. T. B. Tennakoon, J. M. Thomas, W. Jones, T. A. Carpenter and S. Ramdas, *J. Chem. Soc., Faraday Trans. 1*, 1986, **82**, 545.
10 M. S. Baksh, E. S. Kikkinides and R. T. Yang, *Ind. Eng. Chem. Res*., 1992, **31**, 2181.
11 E. Gutierrez and E. Ruiz-Hitzky, in *Molecular Rearrangement*

Reactions on Pillared Clays, ed. I. V. Mitchell, Elsevier Applied Science, Barking, 1990, p. 199.
12 K. Urabe, N. Kouno, H. Sakurai and Y. Izumi, *Adv. Mater*., 1991, **3**, 558.
13 J. Sterte, *Clays Clay Miner*., 1991, **39**, 167.
14 D. Y. Zhao, Y. S. Yang and X. X. Guo, *Inorg. Chem*., 1992, **31**, 4727.
15 S. Yamanaka, Y. Inoue, M. Hattori, F. Okumura and M. Yoshikawa, *Bull. Chem. Soc. Jpn*., 1992, **65**, 2494.
16 S. Ghosh, P. Mukundan, K. G. K. Warrier and A. D. Damodaran, *J. Mater. Sci. Lett*., 1991, **10**, 1193.
17 S. Sivakumar, K. G. K. Warrier and A. D. Damodaran, *Polyhedron*, 1993, **12**, 2587.
18 A. Gil and M. Montes, *Langmuir*, 1994, **10**, 291.
19 K. Takahama, M. Yokoyama, S. Hirao, S. Yamanaka and M. Hattori, *J. Mater. Sci*., 1992, **27**, 1297.
20 M. D. Alba, R. Alvero, M. A. Castro and J. M. Trillo, in *Study of the Accessible Micropore Volume in Pillared Montmorillonites*, ed. C. A. C. Sequeira and M. J. Hudson, Kluwer Academic Publishers, Dordrecht, 1993, p. 49.
21 J. Sterte, *Clays Clay Miner*., 1986, **34**, 658.
22 F. Gonzalez, C. Pesquera, C. Blanco, I. Benito and S. Mendioroz, *Inorg. Chem*., 1992, **31**, 727.
23 I. Izumi, W. W. Dunn, K. O. Wilbourn, F-R. F. Fan and A. J. Bard, *J. Phys. Chem*., 1980, **84**, 3207.
24 H. Yoneyama, S. Haga and S. Yamanaka, *J. Phys. Chem*., 1989, **93**, 4833.
25 J. Bovey, PhD Thesis, Cambridge University, 1996.
26 J-T. Lin, S-J. Jong and S. Cheng, *Microporous Mater*., 1993, **1**, 287.
27 *Crystal Structures of Clay Minerals and their X-ray Identification*, ed. G. W. Brindley and G. Brown, Mineralogical Society, London, 1980, monograph 5.
28 J. Bovey, F. Kooli and W. Jones, *Clay Miner*., 1996, **31**, 499.
29 J. Bovey and W. Jones, *J. Mater. Chem*., 1995, **5**, 2027.
30 P. B. Malla and S. Komarneni, *Clays Clay Miner*, 1993, **41**, 472.
31 J. Wu, E. F. Rakiewicz and R. R. Gatte, *Mater. Res. Soc. Symp. Proc*., 1995, **371**, 181.
32 C. Breen, *Clay Miner*., 1991, **26**, 473.
33 R. Mokaya and W. Jones, *J. Chem. Soc., Chem. Commun*., 1994, 929.
34 A. Bernier, L. F. Admaiai and P. Grange, *Appl. Catal*., 1991, **77**, 269.
35 H. L. Del Castillo, A. Gil and P. Grange, *Catal. Lett*., 1996, **36**, 237.
36 H. L. Del Castillo and P. Grange, *Appl. Catal. A: General*, 1993, **103**, 23.
37 R. Swarnakar, B. B. Kerstin and K. A. Kydd, *Appl. Catal. A: General*, 1996, **142**, 61.
38 S. Chevalier, R. Franck, H. Suquet, J. F. Lambert and D. Barthomeuf, *J. Chem. Soc., Faraday Trans*., 1994, **90**, 667.
39 S. A. Bagshaw and R. P. Cooney, *Chem. Mater*., 1993, **5**, 1101.
40 S. J. Gregg and K. S. W. Sing, *Adsorption, Surface Area and Porosity,* Academic Press, London, 1982.
41 R. Mokaya, PhD Thesis, Cambridge University, 1992.
42 E. P. Parry, *J. Catal*., 1963, **2**, 371.
43 M. Lefrançois and G. Malbois, *J. Catal*., 1971, **20**, 350.
44 J. Connerton, R. W. Joyner and M. B. Padley, *J. Chem. Soc., Faraday Trans*., 1995, **91**, 1841.
45 J. A. Ballantine, M. Davies, I. Patel, J. H. Purnell, M. Rayanakorn, K. J. Williams and J. M. Thomas, *J. Mol. Catal*., 1984, **26**, 37.
46 S. M. Bradley and R. A. Kydd, *J. Catal*., 1993, **141**, 239.

Paper 6/04865J; *Received* 10*th July*, 1996